

Electronic Supplementary Information (ESI)

Purification of octafluoropropane from hexafluoropropylene /octafluoropropane mixtures with a metal-organic framework exhibiting high productivity

Yuan-Qin Feng^{1†}, Hui-Fan Ma^{1†}, Shuai Luo¹, Hui-Ping Xiao¹, Qing-Yan Liu^{1,2} and Yu-Ling Wang^{1*}

¹ College of Chemistry and Materials, Key Lab of Fluorine and Silicon for Energy Materials and Chemistry of Ministry of Education, Jiangxi Normal University, Nanchang 330022, China. ² Fujian Provincial Key Laboratory of Eco-Industrial Green Technology, College of Ecology and Resources Engineering, Wuyi University, Wuyishan 354300, Fujian, China. [†] These authors contributed equally.

Corresponding Authors (email: ylwang@jxnu.edu.cn)

1. Characterization.

Physical Measurements. FT-IR spectra were recorded from KBr disc on a Perkin-Elmer Spectrum One FT-IR spectrometer ranging from 400 to 4000 cm⁻¹. Thermogravimetric analyses were performed under a nitrogen atmosphere with a heating rate of 10 °C/min using a PE Diamond thermogravimetric analyser. Powder X-ray diffraction analyses were performed on a Rigaku Ultima IV diffractometer with Cu-K α radiation ($\lambda = 1.5418 \text{ \AA}$).

Crystallographic Study. X-ray single-crystal diffraction experiment was carried out a Bruker D8 Venture diffractometer (Cu-K α radiation, $\lambda = 1.54178 \text{ \AA}$). Absorption correction and data reduction were handled with a *SADABS*.¹ The *SHELXT*² and *SHELXL*³ were applied to structure solution and refinement. The chlorine atom of a 3-chloroisonicotinic ligand were disordered over two positions. Thus the hydrogen atoms of a 3-chloroisonicotinic ligand couldn't be added. All other hydrogen atoms were modelled geometrically and refined with a riding model. Non-hydrogen atoms were refined anisotropically. The guest water and DMA molecules are highly disordered and treated by *SQUEEZE* of *PLATON*.⁴

Isosteric heat of adsorption. The gas adsorption isotherms measured at 273 and 298 K were first

fitted to a virial equation (equation S1) (Fig. S5).⁵ Then the Q_{st} values for C_3F_6 and C_3F_8 were calculated based on the fitting parameters using equation S2.

$$\ln P = \ln N + \frac{1}{T} \sum_{i=0}^m a_i N^i + \sum_{i=0}^n b_i N^i \quad (\text{equation S1})$$

$$Q_{st} = -R \sum_{i=0}^m a_i N^i \quad (\text{equation S2})$$

where P is pressure (mmHg), N is the adsorbed quantity (mmol g^{-1}), T is the temperature (K), a_i and b_i are virial coefficients, R is the universal gas constant (8.314 J K^{-1} mol $^{-1}$), and m and n determine the number of coefficients required to adequately describe the isotherm.

Ideal adsorbed solution theory (IAST) calculations of adsorption selectivity. The IAST was used to predict mixed gas behavior from experimentally measured single-component isotherms.⁶ The experimentally measured loadings for C_3F_6 and C_3F_8 in JXNU-21 were fitted with the single-site Langmuir-Freundlich model (equation S3 and Fig. S6).

$$q = q_{A,sat} \frac{b_A p^{c_A}}{1 + b_A p^{c_A}} \quad (\text{equation S3})$$

Where p (unit: kPa) is the pressure of the bulk gas at equilibrium with the adsorbed phase, q (unit: mmol g^{-1}) is the adsorbed amount per mass of adsorbent, $q_{A,sat}$ (unit: mmol g^{-1}) is the saturation capacity, b_A (unit: 1/kPa) is the affinity coefficient. The c_A represents the deviation from an ideal homogeneous surface site.

The adsorption selectivity for binary mixture (A and B) using the Langmuir fitting parameters is defined by equation S4.

$$S_{ads} = \frac{q_A/q_B}{y_A/y_B} \quad (\text{equation S4})$$

(where the q_A and q_B represent the molar loadings (mmol g^{-1}). The y_A and y_B ($y_B = 1 - y_A$) are the mole fractions in a bulk fluid mixture).

Breakthrough separation experiments. The breakthrough curves were measured on a homemade apparatus for the binary C_3F_6/C_3F_8 ($v:v = 10:90$) at 298 K and 1 bar. The gas flows were controlled at the inlet by a mass flow meter as 4 mL min^{-1} for the binary mixtures. A gas chromatograph (TCD-Thermal Conductivity Detector) continuously monitored the effluent gas from the adsorption bed.

Prior to every breakthrough experiment, we activated the sample by flushing the adsorption bed with helium gas for 1 hours at 298 K. Subsequently, the column was allowed to equilibrate at the measurement rate before we switched the gas flow.

Grand canonical Monte Carlo (GCMC) simulation and Density Functional Theory (DFT) Calculation.

All the grand canonical Monte Carlo (GCMC) simulations were performed by the Materials Studio package. The adsorption sites of C_3F_6 and C_3F_8 at 298 K were obtained from GCMC simulations through the fixed loading task in the Sorption module. The host framework and the guest molecules were both regarded as rigid. The simulation box consisted of four unit cells and the Metropolis method based on the universal forcefield (UFF) was used. The Q_{Eq} derived charges and the ESP charges derived by DFT were employed to the host framework and guest atoms, respectively. The cutoff radius was chosen as 15.5 Å for the Lennard-Jones potential, and the equilibration steps and production steps were both set as 5×10^6 . We first optimized the structure using the DFT method with periodic boundary. The widely used generalized gradient approximation (GGA) with the Perdew-Burke-Ernzerhof (PBE) functional and the double numerical plus d-functions (DND) basis set were used. An accurate DFT Semi-core Pseudopots (DSPP) was employed for the metal atoms. For all DFT calculations, the energy, gradient and displacement convergence criteria were set as 1×10^{-5} Ha, 2×10^{-3} Å and 5×10^{-3} Å, respectively. To obtain the gas binding energy, a gas molecule placed in a supercell with the same cell dimensions was also relaxed as a reference. The static binding energy (at $T = 0$ K) was then calculated using $E_B = E_{(host\ framework)} + E_{(gas\ molecule)} - E_{(host\ framework + gas\ molecule)}$.

Table S1. Physical parameters for C_3F_6 and C_3F_8 .

	C_3F_6	C_3F_8
Molecule size (Å ³)	$4.84 \times 5.07 \times 7.3$	$5.23 \times 5.73 \times 7.6$
Boiling point (K)	245	234
Polarizability ($\times 10^{-25}$ cm ³)	65.9	68.0

Table S2. Crystal structure refinement data.

JXNU-21	
formula	C ₃₀ H ₁₈ Cl ₅ N ₅ O ₁₂ Co ₃
fw	994.53
temp (K)	298(2) K
Radiation	Cu-K α (1.54178 Å)
cryst syst	Monoclinic
Space group	<i>P2₁/c</i>
<i>Z</i>	4
<i>a</i> (Å)	19.5694(6)
<i>b</i> (Å)	13.5608(4)
<i>c</i> (Å)	18.5731(6)
α (deg)	90
β (deg)	92.730(2)
γ (deg)	90
<i>V</i> (Å ³)	4923.3(3)
<i>D</i> _{calcd} (g·cm ⁻³)	1.342
μ (mm ⁻¹)	10.775
no. of reflns collected	44315
independent reflns	8946
<i>F</i> (000)	1980
<i>R</i> _{int}	0.0731
<i>R</i> ₁ (<i>I</i> > 2 σ (<i>I</i>)) ^a	0.0760
<i>wR</i> ₂ (<i>I</i> > 2 σ (<i>I</i>)) ^a	0.2009

It should be noted that the counter ions of hydroxide ions are not included into the formula.

$$^a R_1 = \frac{\sum ||F_o| - |F_c||}{\sum |F_o|} \text{ and } wR_2 = \left\{ \frac{\sum [w(F_o^2 - F_c^2)^2]}{\sum [w(F_o^2)^2]} \right\}^{1/2}$$

Table S3. Selected Bond Lengths (Å) for JXNU-21.^a

Bond	distance	Bond	distance	Bond	distance
Co1–O1	2.096(3)	Co1–O3	2.072(4)	Co1–O4	2.063(4)
Co1–O6	2.073(4)	Co1–N2B	2.201(5)	Co1–N3A	2.150(5)
Co2–O1	2.092(3)	Co2–O2	2.081(4)	Co2–O8	2.082(4)
Co2–O10	2.071(4)	Co2–N4C	2.192(5)	Co2–N5A	2.133(5)
Co3–O1	2.071(3)	Co3–O1W	2.068(4)	Co3–O5	2.075(4)
Co3–O7	2.079(5)	Co3–O9	2.093(4)	Co3–O11	2.095(4)

^aSymmetry codes: A $x, 3/2-y, 1/2+z$; B $2-x, -1/2+y, 3/2-z$; C $1-x, -1/2+y, 3/2-z$.

2. Results and discussion

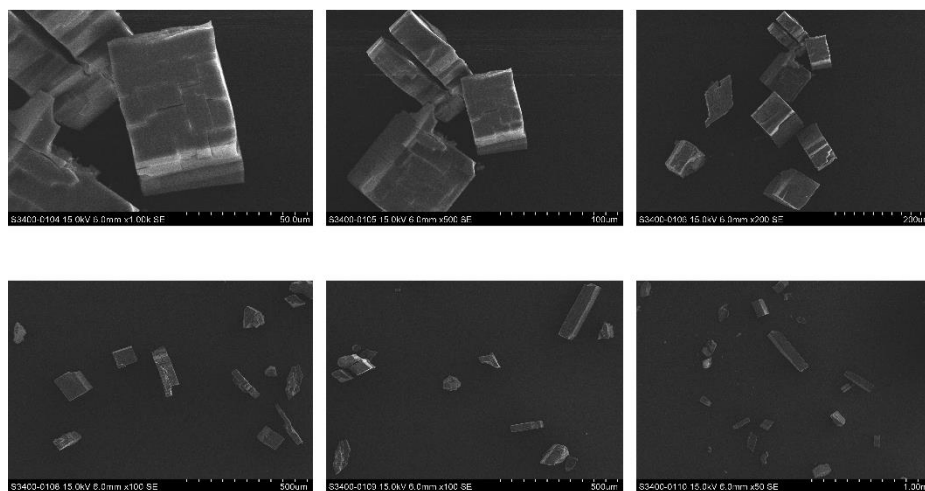


Fig. S1 SEM images for JXNU-21.

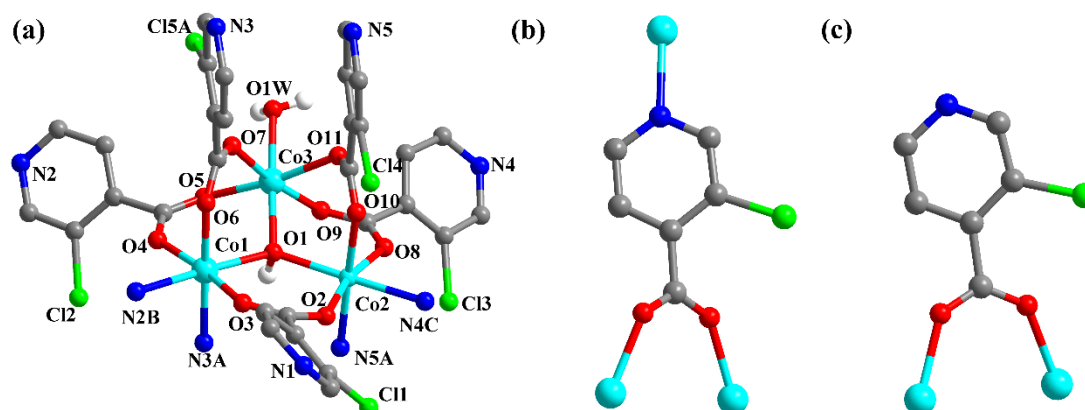


Fig. S2 (a) Coordination environments for Co(II) atoms and (b) and (c) coordination modes of 3-chloroisophthalic ligands and eight isonicotinic ligands.

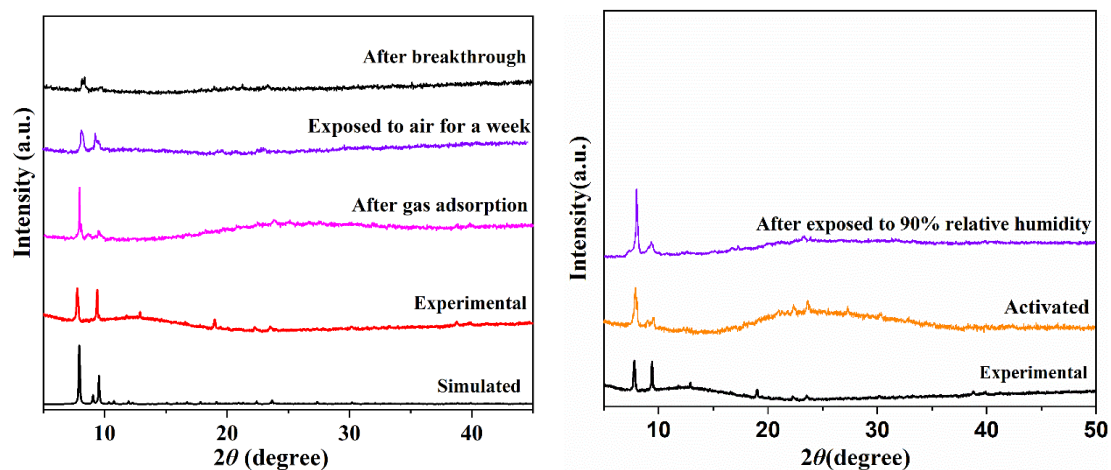


Fig. S3 PXRD patterns of JXNU-21.

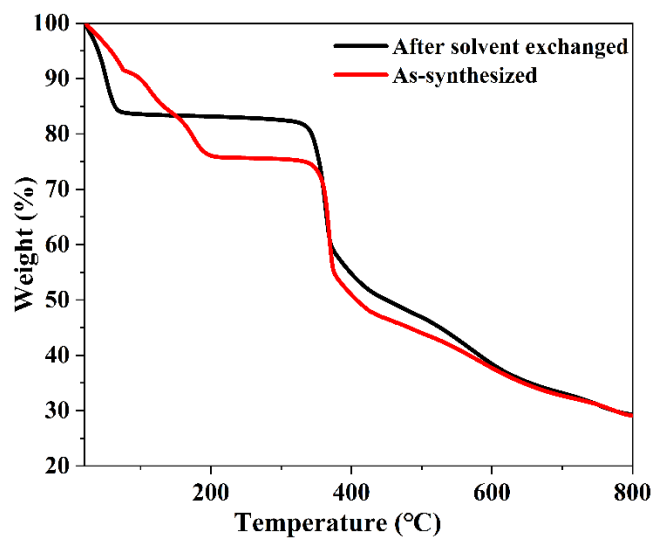


Fig. S4 TGA curves of JXNU-21.

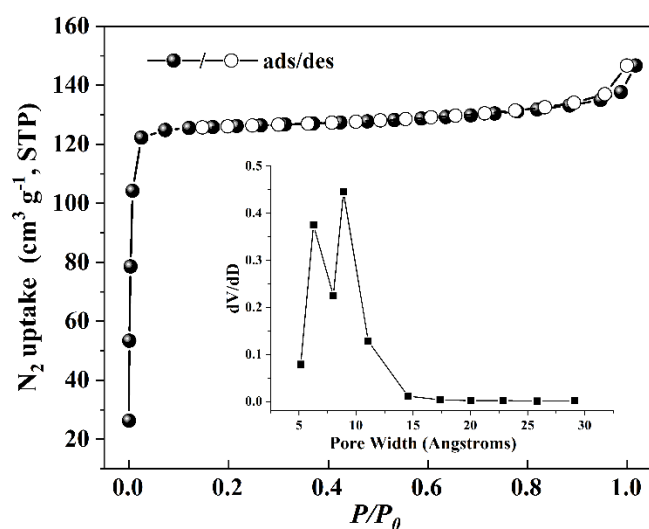


Fig. S5 N₂ adsorption/desorption isotherms for JXNU-21 at 77 K.

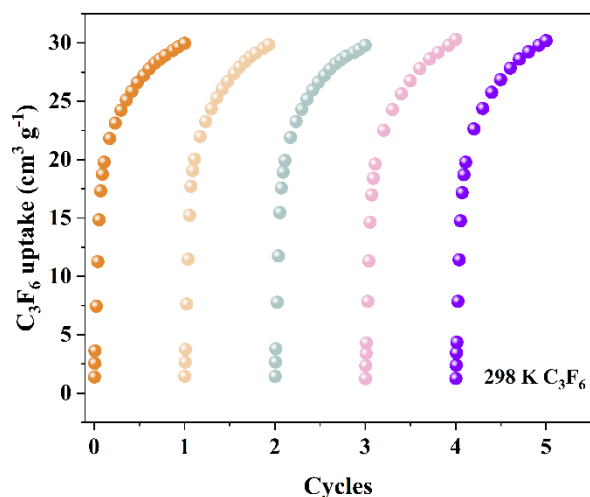


Fig. S6 Five cyclic C_3F_6 adsorption isotherms for JXNU-21 at 298 K.

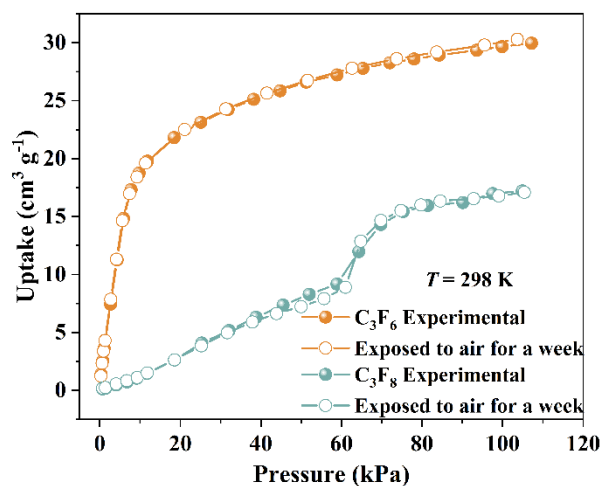


Fig. S7 Comparison of the C_3F_6 and C_3F_8 adsorption isotherms at 298 K for the pristine sample and the sample exposure to air for a week.

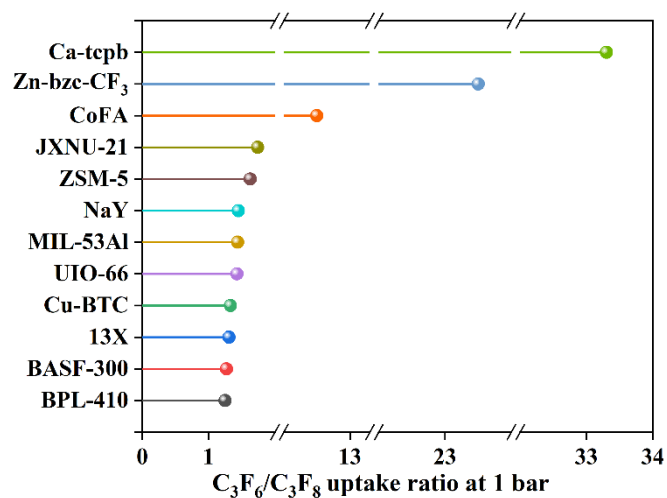


Fig. S8 Comparison of the C_3F_6/C_3F_8 uptake ratio at 1 bar for all sorbents at 298 K.

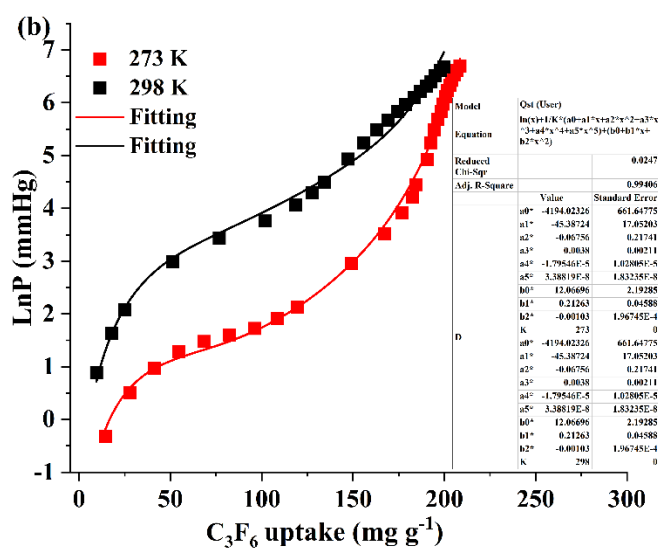
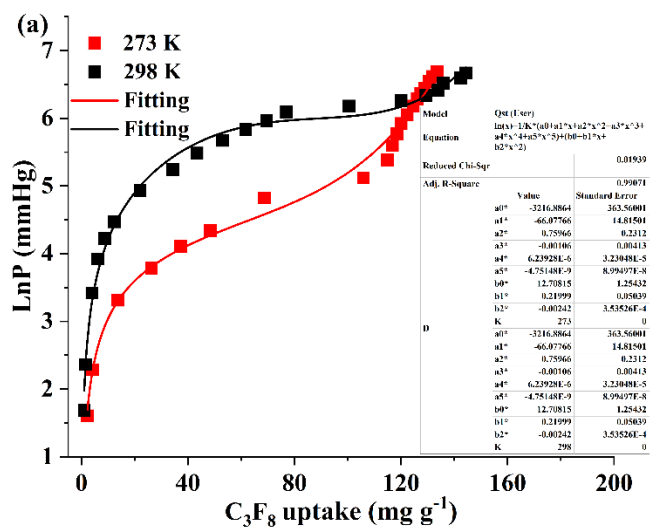
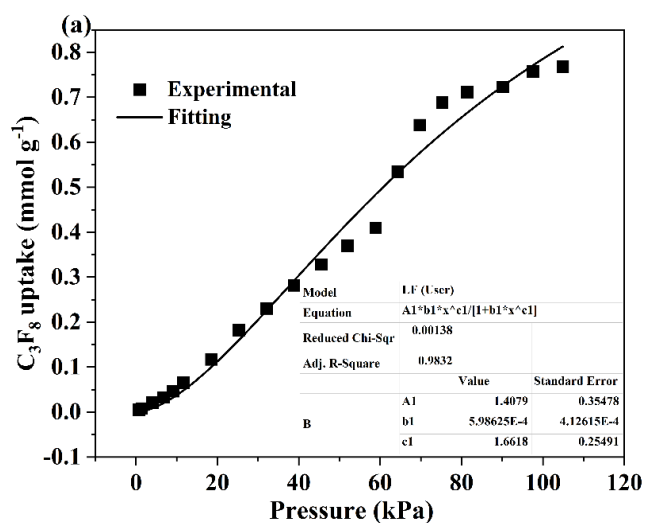


Fig. S9 Virial fits of (a) C₃F₈ and (b) C₃F₆ isotherms for JXNU-21.



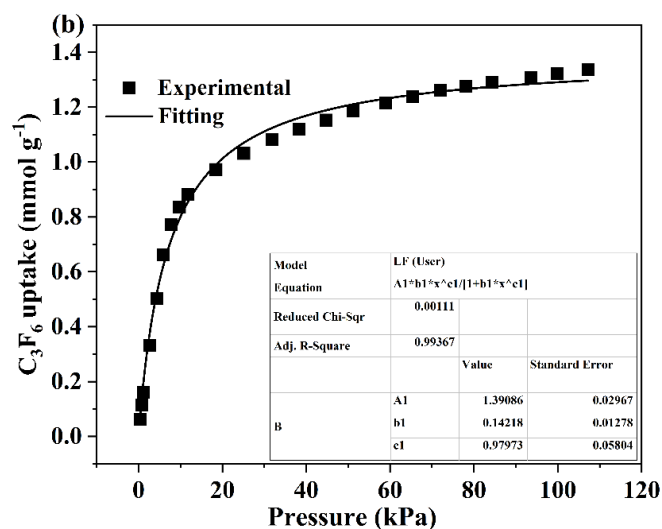


Fig. S10 The graphs of the single-site Langmuir-Freundlich equation fit for adsorption of (a) C_3F_8 and (b) C_3F_6 for JXNU-21 at 298 K.

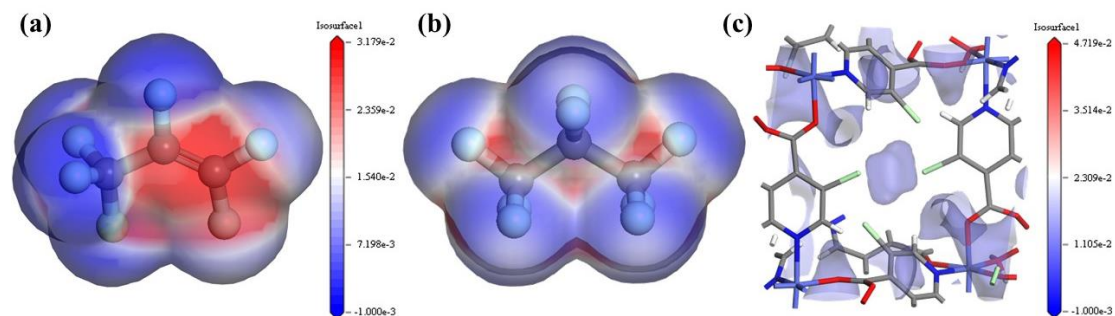


Fig. S11 The calculated surface electrostatic potential of (a) C_3F_6 and (b) C_3F_8 and (c) JXNU-21.

References

- 1 L. Krause, R. Herbst-Irmer, G.M. Sheldrick and D. Stalke, *J. Appl. Cryst.*, 2015, **48**, 3–10.
- 2 G. M. Sheldrick, *Acta Crystallogr. Sect. A Found Adv.*, 2015, **A71**, 3–8.
- 3 G. M. Sheldrick, *Acta Crystallogr. Sect. C Struct. Chem.*, 2015, **C71**, 3–8.
- 4 A. L. Spek, *PLATON: A Multipurpose Crystallographic Tool*; Utrecht University: Utrecht, The Netherlands. 2001.
- 5 J. L. C. Rowsell and O. M. Yaghi, *J. Am. Chem. Soc.*, 2006, **128**, 1304–1315.
- 6 A-L Myers and J. M. Prausnitz, *AIChE J.*, 1965, **11**, 121–127.